ELSEVIER

J. Wind Eng. Ind. Aerodyn. 51 (1994) 319–338

JOURNAL OF wind engineering AND industrial aerodynamics

Wind loading over the top portions of tall stacks with and without external landing platforms

K. Suresh Kumar and G.N.V. Rao*

Department of Aerospace Engineering, Indian Institute of Science, Bangalore 560012, India

(Received January 6, 1992; accepted in revised form July 19, 1993)

Abstract

The variation of the drag force near the top portions of tall stacks with and without external landing platforms, and with the exit open and closed, has been examined by model studies in a wind tunnel at Reynolds numbers of about 10^5. Pressure measurements on three models of different height to diameter ratios have been supplemented by flow visualisation studies. Observations confirm that when there is no platform, significant load enhancement over the top three to four diameters occurs, due to the high suction caused by the sharp separation of the flow over the top from the rim, in the aft regions of the stack. The enhanced loading is found to be greater if the exit is closed. A platform at the top, of less than twice the exit diameter, further increases the drag force near the top, but a still larger platform at the top, of about three times the exit diameter, decreases the drag force to values less than those much further below, effectively nullifying the enhanced drag force. It was found that such a reduction of the enhanced drag force in the top regions can also be achieved by a smaller platform of 1.1 to 1.3 times the local diameter, located at about three to five diameters below the top.

Key words: Wind loading; Tall stacks; External landing platforms; Drag force; Pressure measurements

Notation

C_p	pressure coefficient
C_d	local drag coefficient (drag coefficient at a section)
C_D	average drag coefficient over the top three diameters
Re	Reynolds number
D_t	diameter at the top of the stack model
H	height of the stack model
Y	distance from the top to the pressure tap

*Corresponding author.

SSDI 0167-6105(93)E0044-Y

Y_p distance from the top to the platform
B radial width of the platform
d_1 inner diameter of the platform
d_2 outer diameter of the platform
Z (Y/D_t)
Z_p (Y_p/D_t)

1. Introduction

In 1970, ESDU [1] and later, Okomoto and Yagita [2] reported that the drag coefficients for sections near the top two to three diameters of finite height cylinders were much higher than for those further below. Such load enhancement near the top had also been noticed by Niemann [3] on cooling tower models. Recently, the ACI code for chimneys [4] recommended $C_d = 1.0$ over the top 1.5 diameters and the Indian chimney code just issued has recommended a uniform value of 0.8 over the entire height of the chimney, instead of the usual values of between 0.65 to 0.7 in most codes. Before applying such load enhancement to actual stack design, it is necessary to consider the effect of external landing platforms, of closing of the exit in the case of multiflue stacks, the effect of taper and the effect of plume exhaust. For example, a significant effect of a top landing platform on the across-wind loading of stack models had been noted by Scruton [5] and Krishnaswamy et al. [6]. Landing platforms are provided at the top not only for servicing, but also to prevent "flagging" of the exhaust (Plate 1). The effect of plume exhaust is not studied in this paper. The main object of the present study was to examine the effect of the size and location of landing platforms with exit open and closed. A few preliminary results had been presented earlier [7].

Plate 1. A ventilation stack with a wide top landing platform (Kalpakkam, India).

2. Details of experiment:

All the measurements were made in the 2.75 m × 4.25 m × 6.0 m low speed open circuit wind tunnel of the Department of Aerospace Engineering, Indian Institute of Science, Bangalore. This wind tunnel has a turbulence level of 0.2% and a maximum wind speed of about 300 Km/h.

Three aluminium stack models, of which the details are given in Table 1, were used for this study (Plate 2). Static pressure holes of about 0.5 mm diameter were drilled along four generators at 90° in azimuth, at nine to ten elevations near the top, over a height of about three diameters. The elevations were chosen according to a linear law, so that more stations are located near the top, and the ratio of the distance from the top to the exit diameter varied from 0.038 to 3.000. A PC based Scani-valve system was used for measuring the pressures, and the drag force was obtained by integrating the pressures.

Table 1
Details of the stack models

No.	Height H (cm)	Top dia D_t (cm)	H/D_t	Taper
Model I	111.0	3.90	28.46	1/37.58
Model II	144.5	7.10	20.35	1/49.07
Model III	102.0	3.45	29.56	1/39.62

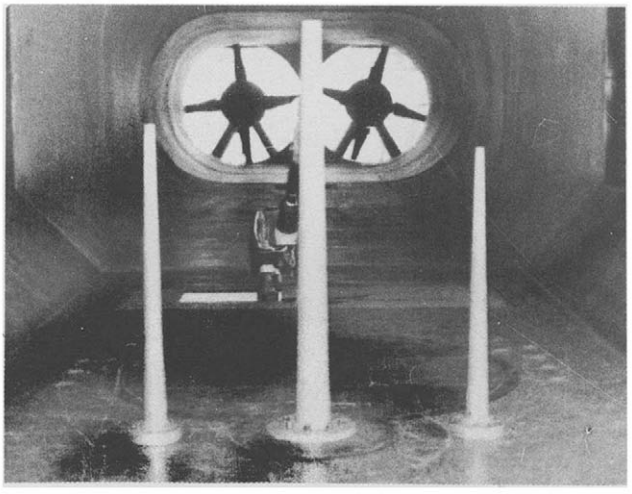

Plate 2. Stack models used in the present study.

The external platforms were simulated by hollowed aluminium discs cut from a 0.5 mm thickness sheet. The ratio of the outer diameter of the stack model at the top to the outer diameter of the landing platform varied from 0.301 to 0.780.

The model was fixed to a turntable mounted on the floor of the wind tunnel, which allowed measurement of C_p at every 10° in azimuth. A total of about 18 configurations (external platforms of different sizes, exit open and closed) were studied for each model. The test Reynolds number, based on the top diameter, varied from about 5.0×10^4 to 2.0×10^5. Flow visualisation studies using a suspension of lampblack powder in kerosene and oil were also made.

3. Results of test programme

Although full results for all the models are available [8], only the main results from one of the models are presented here, to indicate the type of information from which broad conclusions applicable for all the models were drawn. The results without the platforms are first presented and later compared with the results with platforms. Since the positive pressure on the front side and the negative pressure on the back side are good indicators of the drag force, values of C_p at $\theta = 0°$ and 180° in the top regions are also given.

3.1. Drag force without landing platforms

Fig. 1 shows the distribution of the pressure with θ on model 1 at different heights. The variation of C_p at $\theta = 0°$ and 180° is separately given in Figs. 2 and 3. While the

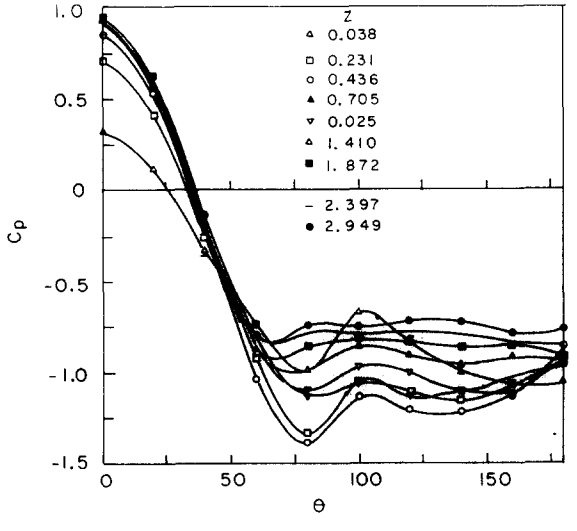

Fig. 1. C_p versus θ (Ist model, exit open, without platform).

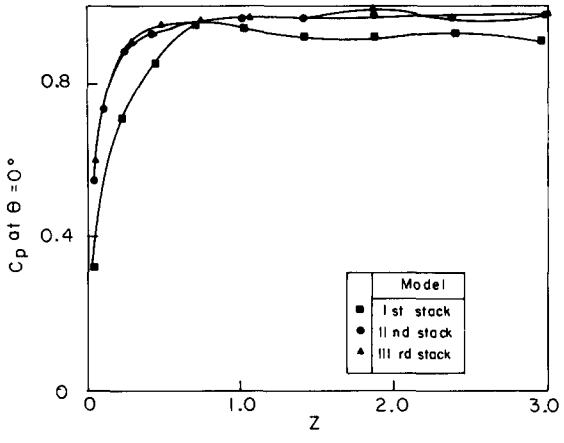

Fig. 2. C_p at $\theta = 0°$ versus Z (all the models, exit open, without platform).

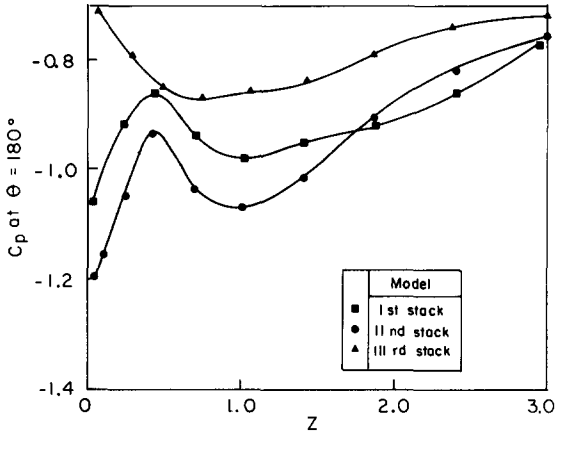

Fig. 3. C_p at $\theta = 180°$ versus Z (all the models, exit open, without platform).

low positive pressures around $\theta = 0°$ very near the top are to be expected [2], the maximum value further down did not reach the stagnation value of 1.0 as in Ref. [2] with straight circular cylinders. There appears to be a tendency to reach an asymptotic value of less than 1.0 below $Z = 0.5$.

The negative values of C_p at $\theta = 180°$ are found to take a longer distance from the top before any tendency to reach an asymptotic value can be discerned. In the case of models 1 and 2, the suction at the back is observed to be much higher over the top 3 diameters than further below. One might conjecture that this is due to the "sharp" separation of the flow from the rim at the top, as against the "smooth" boundary layer separation [9] in regions well below the top. The negative pressure at the rear initially

decreases with distance down from the top to about $Z = 0.5$, below which there is an increase again of negative pressure down to about $Z = 0.9$. Below $Z = 0.9$, there is a gradual decrease in negative pressure, and it appears that the value stabilises at around -0.75 below $Z = 3.0$. However, in the case of model 3, the suction increases down to $Z = 0.5$, below which the pressure gradually increases and appears to stabilise again at -0.75. Such variations have also been observed by others [3].

Plate 3 shows a clear laminar separation line at $\theta = 90°$ (flow is from right to left). It is also observed that the laminar separation line close to the top, is pushed downstream up to an angle of about 130°.

The value of the local drag coefficient C_d at each level from the top, is presented in Fig. 4 for all the three models. It is observed that the peak C_d occurs between $Z = 0.3$ and $Z = 0.7$ for all the models. It is clear that the peak C_d and its average C_D, given in the table appended to Fig. 4, depend on (H/D). Another result to be noted is that in all the three models, C_D is equal to or greater than unity, but not equal to the subcritical Re value of 1.2 for an infinite circular cylinder.

3.2. *Models with exit closed and without platforms*

The corresponding values of C_p at $\theta = 0°$ and 180° with the exit closed, and with no landing platforms are given in Figs. 5 and 6. The distribution of C_d at different

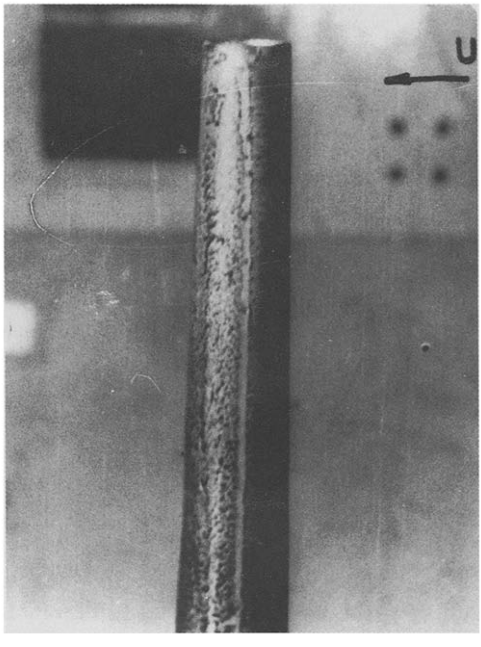

Plate 3. Flow pattern near the top of model I with exit open and with no landing platform showing a clear separation bubble at the top.

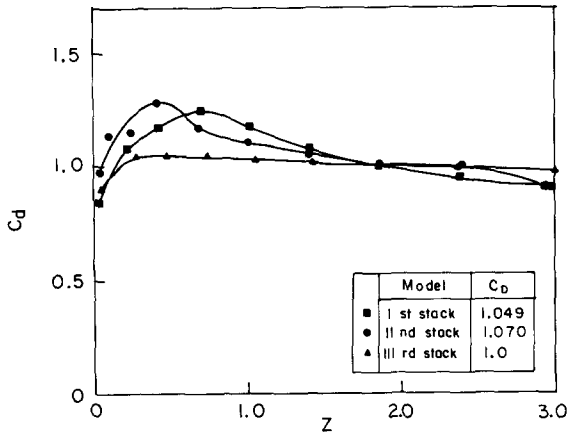

Fig. 4. C_d versus Z (all the models, exit open, without platform).

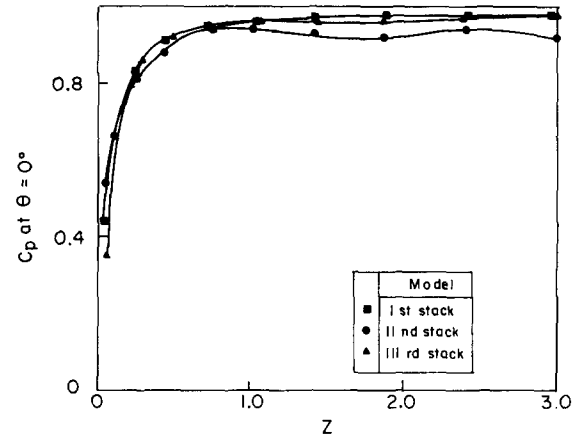

Fig. 5. C_p at $\theta = 0°$ versus Z (all the models, exit closed, without platform).

distances from the top is given in Fig. 7. It is observed that while the C_p distribution at $\theta = 0°$ takes a longer distance of about one diameter from the top to show any tendency to stabilise, the pressures at $\theta = 180°$ show a different variation with height. The values of C_d at various distances from the top (Fig. 7) are found to be higher in all the three models compared to the values with the exit open (Fig. 4). Similar results are observed for C_D (Tables appended to Figs. 4 and 7).

3.3. *Models with platforms of different diameters at the top*

The second series of experiments were made with platforms of different diameters at the top only. The pressure values at $\theta = 0°$ and $\theta = 180°$, presented in Figs. 8 and 9,

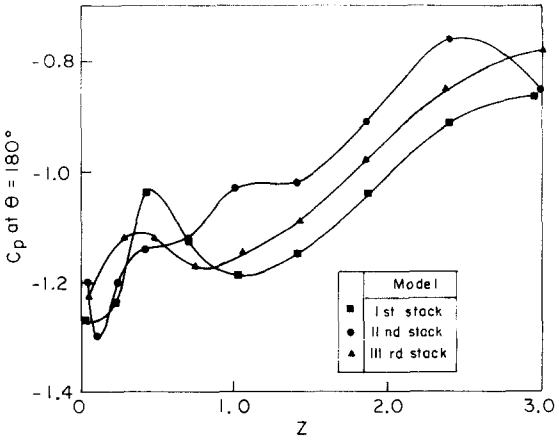

Fig. 6. C_p at $\theta = 180°$ versus Z (all the models, exit closed, without platform).

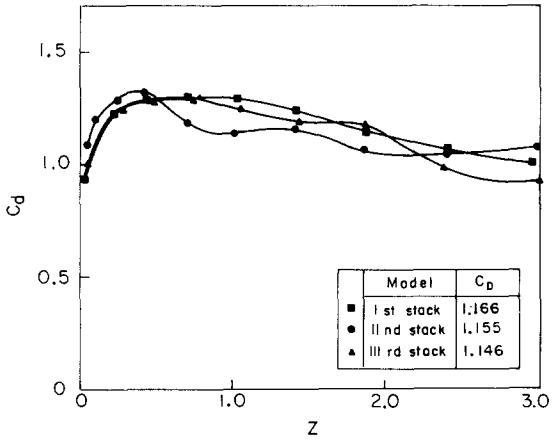

Fig. 7. C_d versus Z (all the models, exit closed, without platform).

show that positive C_p values near the top are not only much higher than the values when there is no platform, as is to be expected, but interestingly, are slightly less than 1.0. It may also be observed that C_p at $\theta = 0°$ (Fig. 8) is nearly insensitive to the size of the platform, at least for (d_1/d_2) values > 0.3. But the back pressure at $\theta = 180°$ (Fig. 9) shows a considerable effect of the size of the platform, which suggests that no two-dimensional flow is produced by the platforms used.

Fig. 10 gives the distribution of C_d with Z for the first model with 1.0 cm to 4.0 cm radial width platforms $(d_1/d_2) = 0.661$ to 0.328, respectively. It is observed that C_d is generally higher for the platforms of 1.0 cm and 1.5 cm radial width compared to the

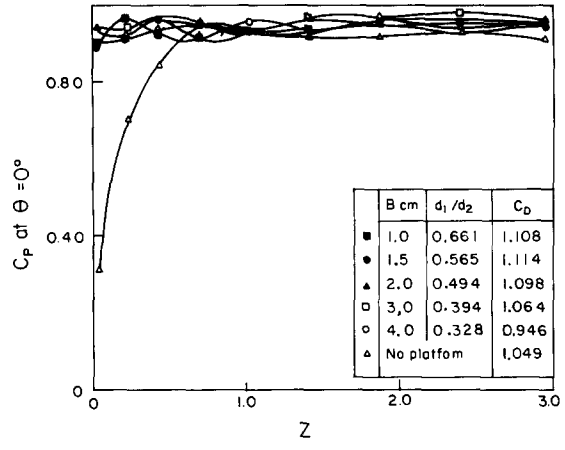

Fig. 8. C_p at $\theta = 0°$ versus Z (Ist model, exit open, B-varying, $Z_p = 0$).

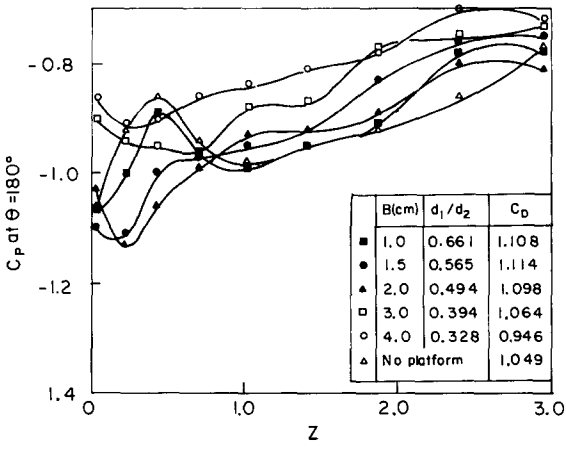

Fig. 9. C_p at $\theta = 180°$ versus Z (Ist model, exit open, B-varying, $Z_p = 0$).

values without the platforms (Figs. 4 and 7). However, (the average) C_D for the 3.0 cm and 4.0 cm radial width platforms is significantly lower than the corresponding value without the platform, showing that the local drag coefficient peaks for a certain size of top platform. The consolidated variation of C_D with (d_1/d_2) with the exit both open and closed, shown in Fig. 11, indicates that C_D reaches a maximum when the ratio (d_1/d_2) is about 0.65 for both the exit open and closed cases, and then decreases to values less than those without any platform. The higher values with the exit closed may also be noted.

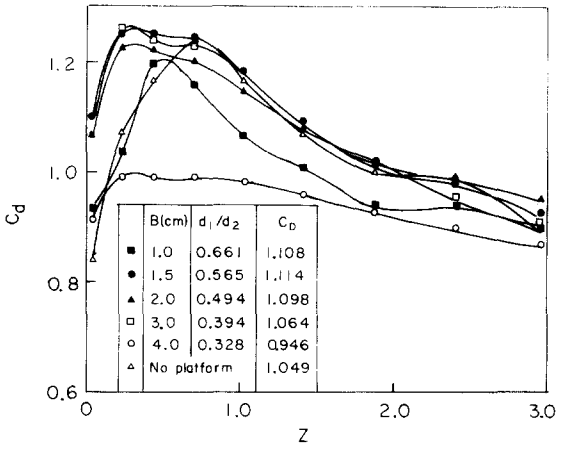

Fig. 10. C_d versus Z (Ist model, exit open, B-varying, $Z_p = 0$).

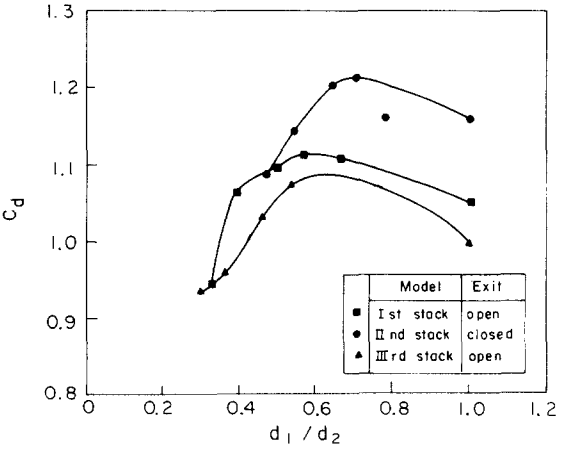

Fig. 11. C_D versus d_1/d_2 (all the models, $Z_p = 0$, B-varying).

3.4. *Effect of 1.0 cm radial width platforms at different distances from the top*

Additional tests were carried out with 1.0 cm radial width platforms at different distances from the top (since this size corresponds to a practical platform width of 1.0 m at the normally used scale of 1:100). The results with model 1 are presented mainly for the case with the exit open since the broad conclusions were found to be the same for all the other models even with the exit closed.

The variation of C_d for different positions of the platform is shown in Figs. 12 and 13, where the total drag coefficient C_D is also indicated in the table appended to the

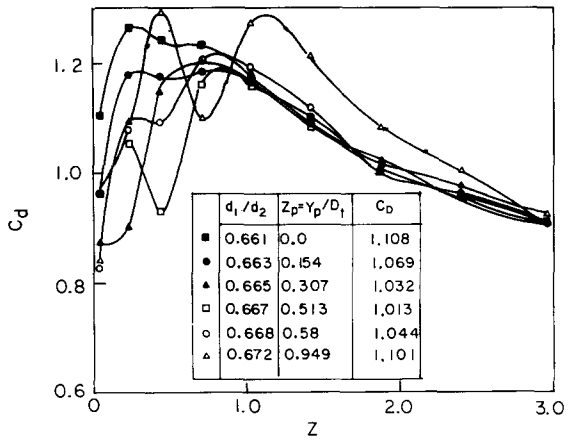

Fig. 12. C_d versus Z (Ist model, exit open, $B = 1.0$ cm, Z_p varying).

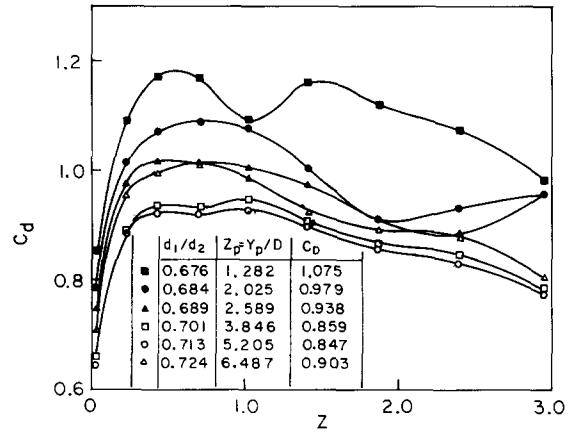

Fig. 13. C_d versus Z (Ist model, exit open, $B = 1.0$ cm, Z_p varying).

graphs. Although the platform was shifted to a position as far below as $Z_p = 6.483$, the C_D values are still the averages over a height of three diameters only. The oil flow pattern below the platform in plate 4 shows a large bubble over a range of θ from 85° to 120° and "clean" separation of flow above the platform at an angle of about 90°. These results seem to imply that there are no trailing vortices at these Re[1].

A consolidation of the total C_D at different positions of the platform on the three models is presented in Fig. 14. All these results are more fully discussed in the next Section.

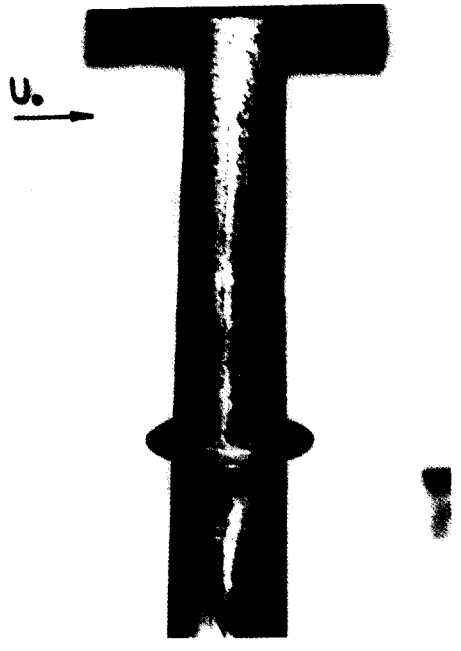

Plate 4. Flow pattern in the top regions of model I with a 1.0 cm platform at $Z_p = 6.5$.

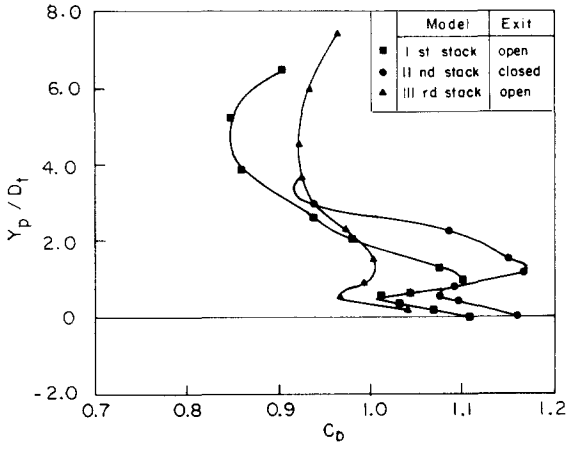

Fig. 14. Y_p versus C_D (all the models, $B = 1.0$ cm, Z_p varying).

4. Discussion of results

4.1. Models with no platform

It seems clear from the results presented above, that the higher drag force in the top region of finite height stacks, is due to the suction of the separation bubble leaving sharply from all round the rim at the top being higher than that of the smoothly separating boundary flow further below. The influence of the higher suction is felt over a region several diameters from the top. Part of the flow moving towards the top under the influence of this higher suction, meets the flow spilling out from the exit of the stack and going downwards, and creates the small secondary bubble seen near the top (Plate 5). The positive value of C_p lower than unity at the front, seems to be due to the taper of the stack.

These observations suggest several possible complex flow patterns, some of which have been sketched in Figs. 15 and 16 for the cases with the exit open and closed, respectively. With the exit open, the separating portion of the front contact line may be swallowed inside the stack or just meet the downstream rim, or "jump" the exit and re-attach below the rim on the rear side. Such behaviour may be expected to depend on taper. H/D and Re. The appearance in Plate 6 (taken from the rear) of a barely visible white patch at the rear side, at a value of Z of about 0.5, could possibly be

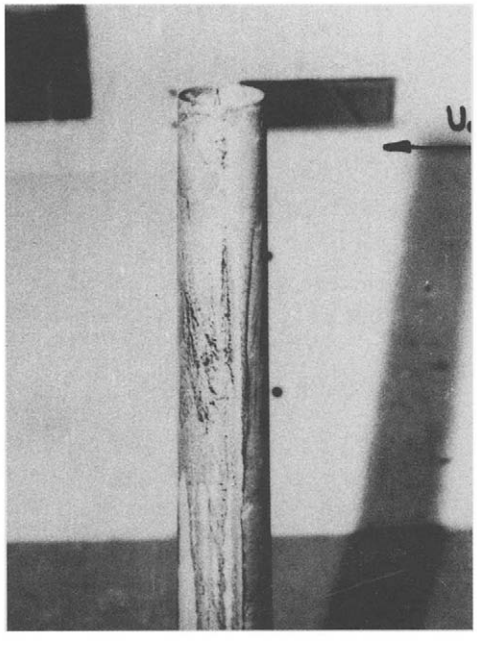

Plate 5. Flow separation pattern on model III near the top with no landing platform showing large separation bubble at the top.

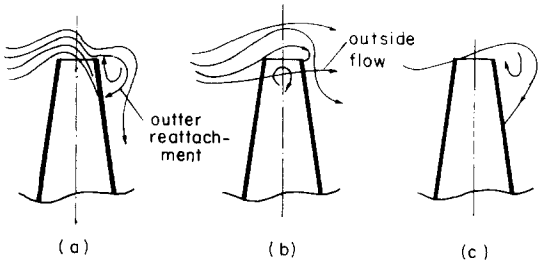

Fig. 15. Possible flow patterns over the top portion of a stack with exit open and without platform.

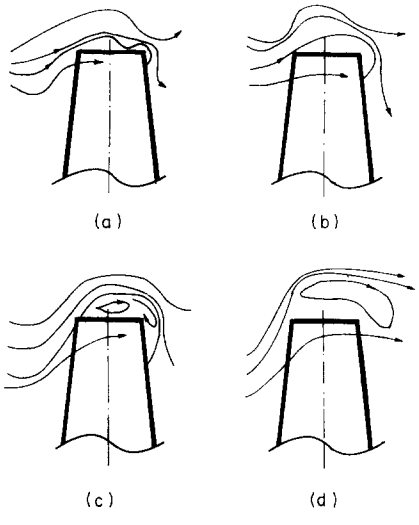

Fig. 16. Possible flow patterns over the top portions of a stack with exit closed and without platform.

interpreted as the zone of turbulent reattachment. Similar observations seem to be applicable when the exit is closed.

4.2. *Models with platforms at the top only*

One observes in Figs. 8 to 13 that provision of a platform at the top results in a large increase of C_p at $\theta = 0°$ at and near the top, compared to the case without the platform. The increase is found to be about the same for all radius ratios (d_1/d_2) below about 0.728, indicating that even a small platform at the top can restrict the upward flow sufficiently to increase substantially the positive pressure around $\theta = 0°$.

The surface flow patterns with platforms in Plates 7, 8, 9, and 10 indicate that the flow separates from the rim of the platform on the front side, and seems to re-attach itself inside the stack if the exit is open, but the flow outside the reattachment point climbs out and separates again at the rear rim of the stack. This seems to be the

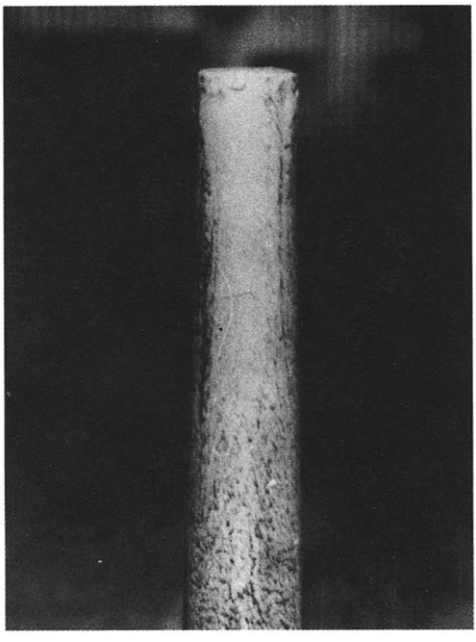

Plate 6. Flow pattern at the rear of model I showing a white patch at about half the top diameter below the top, indicating possible flow reattachment.

Plate 7. Flow pattern over the top of 1.0 cm wide landing platform at the top of model I showing lampblack accumulation over the whole region indicating total flow separation.

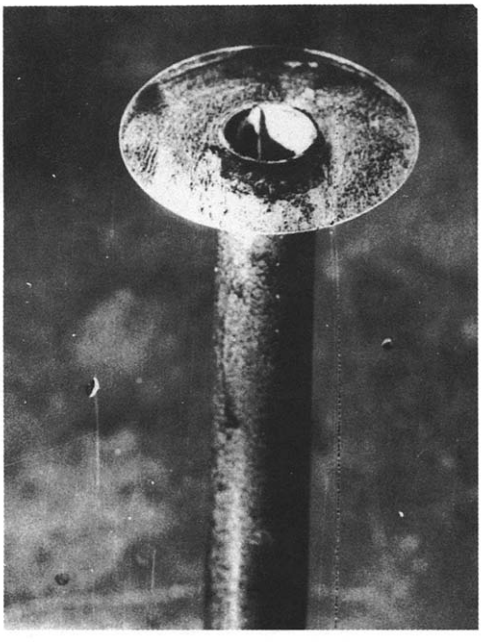

Plate 8. Flow pattern on top of a 4.0 cm wide landing platform ($d_1/d_2 = 0.328$) at the top showing lampblack accumulation at the front and just downstream of the exit.

Plate 9. Flow pattern over the top of model I with exit closed and 1.0 cm wide platform ($d_1/d_2 = 0.661$) showing reattachment of flow on the closing diaphragm.

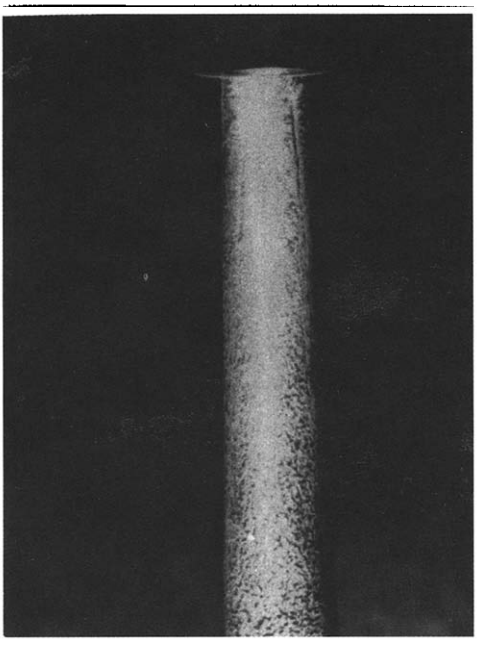

Plate 10. Flow pattern at the rear of model I showing the trace of the separation line at the top is reached in the presence of a landing platform.

behaviour when the platform radius is not large, if one may interpret the more or less total coverage of the top of the platform by lampblack in Plate 7 taken along the flow direction. The pattern with the large radius platform in Plate 8, also taken along the direction of flow looking downstream ($\theta = 0°$), suggests a somewhat similar mechanism, except that the lampblack accumulates near the rim of the stack on the upstream side. The emerging flow from the rear rim of the exit seems to jump the rear rim of the platform, with some reverse flow near the rear rim. The flow pattern when the exit is closed may be inferred from Plate 9, which was taken from the downstream side, and suggests that the separated flow at the front rim re-attaches on the closing diaphragm and leaves from the rear rim.

One other observation concerning the flow pattern is also of interest. Plate 9 shows two very distinct separation lines in the vertical direction, near the top, below the platform, with the angle increasing rapidly up to nearly 150° just below the platform, for a platform width $(d_1/d_2) = 0.728$. As the platform size increases, the region of attached flow near the top, below the platform, decreases, as may be seen in Plate 10. Plate 11, with a large platform, does not show any such significant downstream shift of the separation point below the platform.

Accepting the premise that the main reason for the increase in drag near the top, is due to the communication of the much higher suction of the separation bubble at the top, to the rear regions of the stack near the top, one would expect a smaller radius platform to be less effective than a larger radius platform in preventing such

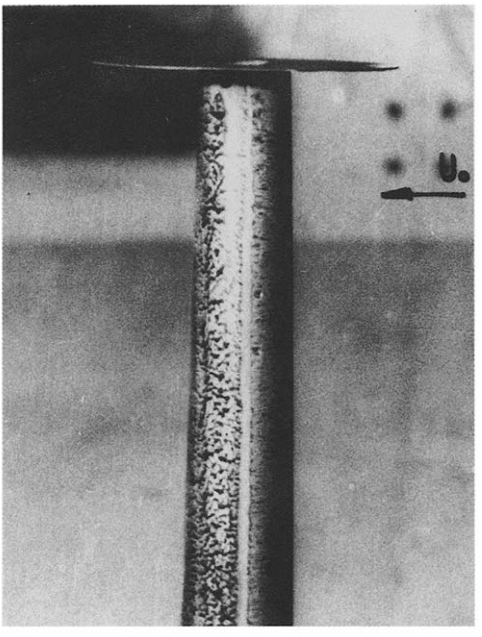

Plate 11. Flow pattern below the wide landing platform at the top showing almost no shift in the separation line along the height.

communication to regions below the top. This explanation, together with the observed high positive C_p values at the front, even when there is a small platform at the top, satisfies the observed higher value of C_D (Fig. 10) with smaller platforms, although the rearward shift of the separation point below the platform (Plate 9), which is also due to the attraction of the high suction near the top, would have decreased C_D to some extent. When the size of the platform is increased, the communication of the higher suction pressure to the aft regions of the flow near the top, below the landing platform and elsewhere, is more effectively hindered, and results in a decrease in drag coefficient. With further increase in platform size, conditions closer to that of a large end plate at the top may be approached, which will lead to $C_D = 1.2$. These observations suggest that there may be a platform size at which the drag coefficient near the top (C_d or C_D) reaches a minimum, possibly less than the values without the platform. Fig. 11 indicates that this happens when (d_1/d_2) is about 0.3.

4.3. Models with 1.0 cm wide platform at different distances from the top

With a 1.0 cm radial width platform, one observes a downstream shift of the separation line over a height of about 0.25 of a diameter just below the platform, at all platform positions. But the separation line above the platform remains surprisingly "two-dimensional" (Plate 4) over a large portion. A study of the distribution of C_d for different positions of the platform, given in Figs. 12 and 13, shows the change in the

pattern as the platform is crossed. The most interesting observation of C_D (Fig. 14) for all the models, is that, initially, it decreases as the platform is moved downwards to about $Z_p = 0.513$, then increases as the platform is moved further down to $Z_p = 0.949$, and then decreases to a value even less than the value without the platform, when the platform is moved further down.

The explanation for the observed variation of C_D with Z_p seems to be as follows. When the 1.0 cm wide platform is at the top, the high suction pressure of the top separation bubble is partially communicated to the rear region of the portion below the platform, because the radial size of the platform is not high enough to shield it fully. Together with the much higher value of positive C_p on the front, this results in higher C_D than when there is no platform at the top. As the platform is moved downwards, the region above the platform becomes similar to that of a stack without the platform, with low positive C_p on the front side. This low value of positive C_p may be expected to result in lower C_d above the platform, than the values when there was a platform at the top. Below the platform and at small distances from the top, the higher positive C_p on the windward side and the continued influence of the high suction at the top, will result in much higher drag than if there was no platform. Initially, it may be observed that the decrease in C_d above the platform is more than the increase of C_d below the platform, and there is, therefore, a net decrease in C_D up to $Z_p = 0.5$. When the platform is moved further down, the value of C_d in the portions "evacuated" by the platform increase to values more than those when that region was below the platform, due to the increased influence of the high suction of the top bubble at the rear (since the shielding by the platform is now absent), and increased positive pressure on the windward side. The net effect is increase of C_D when Z_p is between 0.5 and 1.0. When the platform is shifted further down, the suction pressure in the region below the platform decreases to values less than those when there is no platform, because of the more effective shielding by the platform at the greater distance from the top. The positive C_p values on the front, both above and below the platform, now become comparable to values when there is no platform. These result in a net decrease of C_d compared to values without the platform, particularly below the platform. The total effect is a net decrease in C_D at least over a certain height near the top. One may expect that at a certain value of Z_p, the total C_D in the top regions, will be about the same as the value much further below. Thus one may expect possible neutralisation of the load enhancement over the top region if the platform is properly positioned. Below this optimum position, the presence of a platform is not likely to influence the total drag force. The present results do indicate the possibility of such neutralisation of enhanced loading in the top region, and the optimum position for a 1.0 m full scale radial width platform is found to be about three top diameters below the top.

5. Conclusions

The following conclusions may be drawn from the present study:

(1) The higher drag force over the top three to five diameters of stacks is confirmed.

(2) In the absence of any taper, the ACI value of $C_D = 1.0$ over the top 1.5 diameters seems to be justified, after allowing for the much higher full scale Reynolds numbers of the stacks.

(3) The main reason for the increase of C_D over the top regions is the high suction of the sharp separation bubble coming off from the rear rim at the top, which is communicated downwards upto a distance of at least three diameters.

(4) The drag coefficient near the top is higher by about 10% when the exit is closed, compared to the value when the exit is open.

(5) Radial platforms at the top of up to about twice the outer diameter of the stack at the top, increase the drag coefficient to values much higher than the normal increase. But platforms of still larger diameter, of three times the exit diameter, can completely nullify all the increase in drag force.

(6) Small platforms of about 1.1 to 1.25 times the local diameter of the stack, at a location of three to five exit diameters below the top, can also completely nullify the increased drag force.

References

[1] ESDU-70014, Fluid forces acting on circular cylinders for application in general engineering, part II, Finite length cylinders, October 1970.

[2] T. Okomoto and M. Yagita, The experimental investigation on the flow past a circular cylinder of finite length placed normal to the plane surface in a uniform stream, Bull. JSME, 16(5) (1973) 805–814.

[3] H.J. Niemann, Zur Stationaren Windbelastung Rotation Symmetrischer Bauwerke im Bereich Transleritischer Reynols-zahlen, March 1971.

[4] ACI Standard, ACI 307-88, Standard practice for the design and construction of cast-in-place reinforced concrete chimneys, Detroit, Michigan.

[5] C. Scruton and A.R. Flint, Wind excited oscillations of structures, Proc. Inst. of Civil Eng., 27 (1964) 673–702.

[6] T.N. Krishnaswamy , G.N.V. Rao, S. Durvasula and K.R. Reddy, Wind tunnel model tests of 102 m high MAPP ventilation stack, Kalpakkam, Rep. IWTR 107, 1974, IISc Bangalore 560012.

[7] G.N.V. Rao and K. Suresh Kumar, Some issues concerning enhancement of along-wind and across-wind loads near the top of ventilation stacks of nuclear reactors, SMIRT 11 Trans. Vol. J, August 1991, Tokyo, Japan, pp. 111–116.

[8] K. Suresh Kumar, Effect of landing platforms and exit closure on the drag force near the top portions of tall stacks, MS Thesis, Indian Institute of Science, Bangalore 560012, India, August 1991.

[9] B. Thwaites, Incompressible Aerodynamics, Oxford University Press, 1960, pp. 1152–168.